MOCVD Kinetics and Morphologies of Al_2O_3 Deposits using Aluminum Tri-Isopropoxide(ATI) Precursor

吉川　昇*、高村　修造**、谷口　尚司*、菊池　淳*
Noboru Yoshikawa*, Shuzo Takamura**, Shoji Taniguchi* and Atsushi Kikuchi*

* 東北大学大学院工学研究科金属工学専攻、980-8579宮城県仙台市青葉区荒巻字青葉
** 東北大学大学院生、現在(株)福井村田製作所

* Dept. of Metallurgy, Division of Engineering, Tohoku University, Aramaki, aza-Aoba, Aoba-ku, Sendai,Japan 980-8579

** Graduate student at Tohoku University, Present: at Fukui Murata Inc. Fukui, Japan

Abstract

Aluminum Tri Isopropoxide(ATI) was vaporized and fed into a horizontal tubular reactor with He carrier. Thick film, particles and thin film were obtained in this order from the inlet by thermal atmospheric Chemical Vapour Deposition(CVD). Carbon was detected from the thick film by AES analysis. Exothermic DTA peak at 550K indicated that the particles consisted of $Al(OH)_3$. Exhaust gas from the reactor was analyzed by means of gas-chromatography, and C_3H_6 and C_3H_7OH were detected. As the reactor temperature increased, the concentration of C_3H_6 increased and that of C_3H_7OH decreased.

According to the reaction mechanism suggested in the literature, formation of the obtained deposits was interpreted as follows: The hydrolytic reaction occurred immediately at the inlet low temperature region, depositing thick films containing organics. $Al(OH)_3$ molecules or clusters were formed in the gas phase, either by pyrolytic reaction generating C_3H_6 or by hydrolytic reaction generating C_3H_7OH. Most of the $Al(OH)_3$ molecules or clusters coagulated and particles were formed, on the other hand, remaining molecular $Al(OH)_3$ migrated to the substrate and amorphous Al_2O_3 thin films deposited via surface reaction.

Keywords : MOCVD, Al_2O_3, kinetics, morphology, tubular reactor

I, Introduction

In order to fabricate Al_2O_3 films, Chemical Vapour Deposition(CVD) process has been widely undertaken, because of high producibility and excellent surface coverage[1,2]. Al_2O_3 films are utilized for different applications, such as for hard coatings and for protective coatings of the structural materials against corrosion. On the other hand, they are used for the insulation layer in the electronic devices. Metal organic precursors(MO) are extensively used in these area, because it is possible to deposit the films by thermal CVD at much lower temperature than the cases of conventional chloride precursors. Aluminum Tri Isopropoxide(ATI, $Al(OC_3H_7)_3$) has been one of the most frequently utilized MO precursor, because of relatively high vapour pressure, safety and easiness in handling.

There are number of studies performed so far concerning on the film fabrication[3-8] and the film properties [9,10] such as electric conductivity, dielectric constants, refractive indexes, etc. However, studies on the reaction mechanisms and the kinetics have been limited to few cases[11-13], comparing with the other alkoxide precursors[14], such as tetra-etoxysilane (TEOS) for deposition of SiO_2[15-17].

The reaction mechanism for deposition of Al_2O_3 from ATI was proposed by Schulmann et al.[12] and was expressed by the following sets of reactions:

$$Al(OC_3H_7)_3 + 3H_2O = Al(OH)_3 + 3C_3H_7OH \quad (1)$$

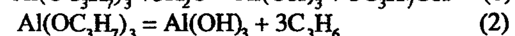

$$Al(OC_3H_7)_3 = Al(OH)_3 + 3C_3H_6 \quad (2)$$

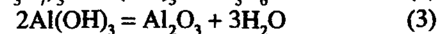

$$2Al(OH)_3 = Al_2O_3 + 3H_2O \quad (3)$$

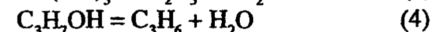

$$C_3H_7OH = C_3H_6 + H_2O \quad (4)$$

The authors have done number of researches on CVD kinetics in relation with microstructure formation, using a horizontal tubular reactor. This reactor configuration has been selected, because of simple gas flow conditions which are suitable for the analysis of deposition kinetics. So it is possible to discuss[18,19] the morphological changes along the axial direction in relation with the reaction kinetics.

In this study, ATI is vaporized and fed into a horizontal tubular reactor, deposits are obtained by atmospheric thermal CVD. The morphologies of the deposits are observed and the film growth rates are measured at different positions in the reactor. Various

techniques were employed for the analysis of the deposits. It is intended to investigate the relationship between the reaction kinetics and the formation of deposits' morphologies from these results. Deposits at different reactor positions are discussed, considering the reaction mechanism shown above.

II, Experimental

The schematic illustration of the apparatus is shown in Fig. 1. They are composed of He gas paths, a vaporizer, a reactor tube and the gas exhaust paths. Vaporized ATI was transported into the reactor with He carrier. Gas of He was selected in order to obtain the higher sensitivity in the gas chromatograph analysis. The output gas was directly fed into a gas-chromatograph and the gas compositions were analyzed. The reactor was sustained horizontally, which was made of stainless steel tube of type SUS304, having inner diameter of 10mm and a slit of 3mm in width, as shown schematically in Fig. 2. Pieces of polished Si wafer were placed in the bottom of the reactor to seal the slit, and the deposits were obtained on the surface of Si wafer. There were temperature distribution along the axial direction of the reactor, as shown in Fig. 3. In this article, the maximum (setup)temperature in the distribution is called the deposition temperature(T). Thickness of the deposited thin film was measured using the interference optical microscope. The thickness was calibrated, comparing with the surface profile measuring system(DEKTAK, Veeco Inc.). Deposition was conducted under the conditions listed in Table 1. The deposits(particles, thick and thin films) were observed by means of scanning electron microscope(SEM). Their compositions were analyzed with Auger electron spectroscopy(AES). Differential thermal analysis (DTA) was made for the deposited particles and for the thick films to investigate the structural changes as the increase of temperature.

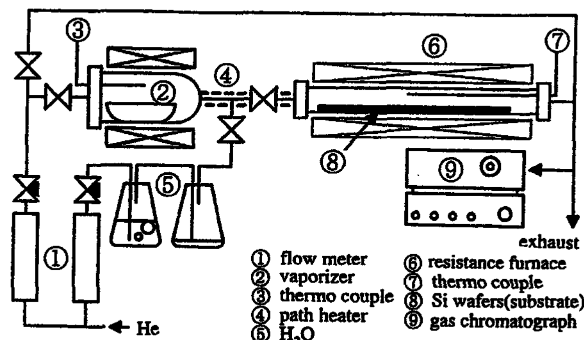

Fig. 1: Schematic illustration of the experimental apparatus.

Table 1. Experimental conditions

Deposition time / ks	3.6
Deposition Temperature / K	573~723
Process Pressure	Atmospheric Pressure
Total Gas Flow Rate / $10^{-6}m^3s^{-1}$	3.3~6.7
ATI Partial Pressure / kPa	0.79~2.27

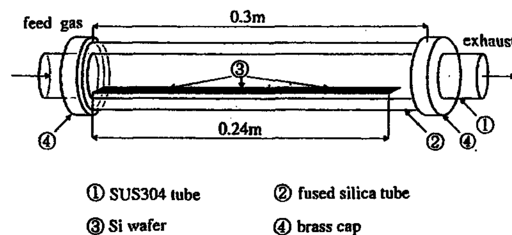

Fig. 2: Schematic illustration of a horizontal tubular reactor.

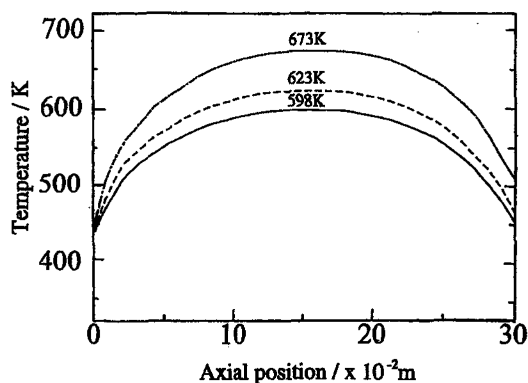

Fig. 3: Temperature distributions along the axial direction of the reactor under different setup temperature(T).

III, Results

[1], Observation of the morphology and analysis of the deposits

1-1 Observation with SEM

SEM photographs shown in Fig. 4 were taken from the deposits at different positions in the tubular reactor. From the inlet, following deposits were observed along the axial direction: thick film, particles(a), particle and film co-deposition(b) and thin film(c). There were large particles of several tens of micrometer in scale which fell on the thick films. Size of the particles decreased along the downstream direction. Particles also deposited in the exit area, however, there was a zone of several centimeters with no deposition, between the thin film deposition region and the exit area. Thickness of

the thick film at the inlet region was of several tens of micron meter and that of the thin film was several hundred nano meter. SEM photographs in Fig. 5 show the surface(a) and the cross section(b) of the thick films. After heating to 600K, the film cracked, as shown in Fig. 5(c).

Co-deposition of particles and film occurred in the intermediate region(Fig.4(b)). Spaces between the particles were filled and the stacks of the particles were densified. This deposition state is similar to that of the CVI process, and quantitative analysis of the co-deposition process has been conducted[20].

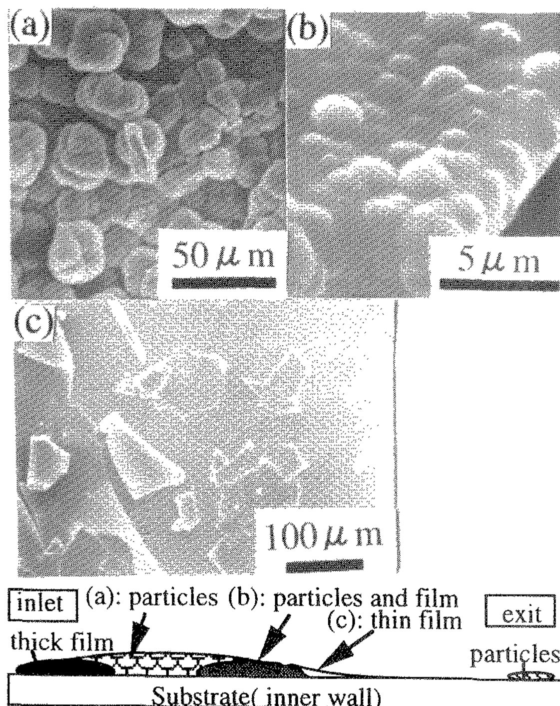

Fig. 4: SEM photographs and the schematic illustration of the deposits(T=623K) on the substrate.

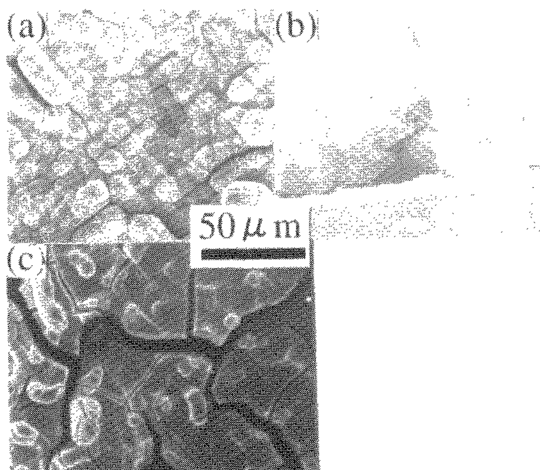

Fig. 5: SEM photographs of the surface(a), cross section of the thick film(b)(deposited at 450~500K) and the surface of the thick film heated to 600K(c).

1-2 Analysis of the deposits

Compositions of the deposits were analyzed by means of AES. In addition to aluminum and oxygen, carbon existed in the sputtered surface of the thick film, as an AES profile shown in Fig. 6(a). No carbon was detected both from the particles(obtained at 0.04m from the inlet) and from the thin films, as shown in Fig. 6(b)(c). DTA profiles from the deposits are shown in Fig. 7 with the solid lines. They are compared with the curves with broken lines, which were obtained from the $Al(OH)_3$ powders(taken as the standard; Wako Chem. Inc.). The exothermic peaks at 380K in Figs. 7(a),(b) were due to desorption of water. The exothermic peaks at 550-600K in Figs. 7(a)(b) were due to transformation from $Al(OH)_3$ to Al_2O_3. Peaks were observed from the standard $Al(OH)_3$ powder at the same temperature region.

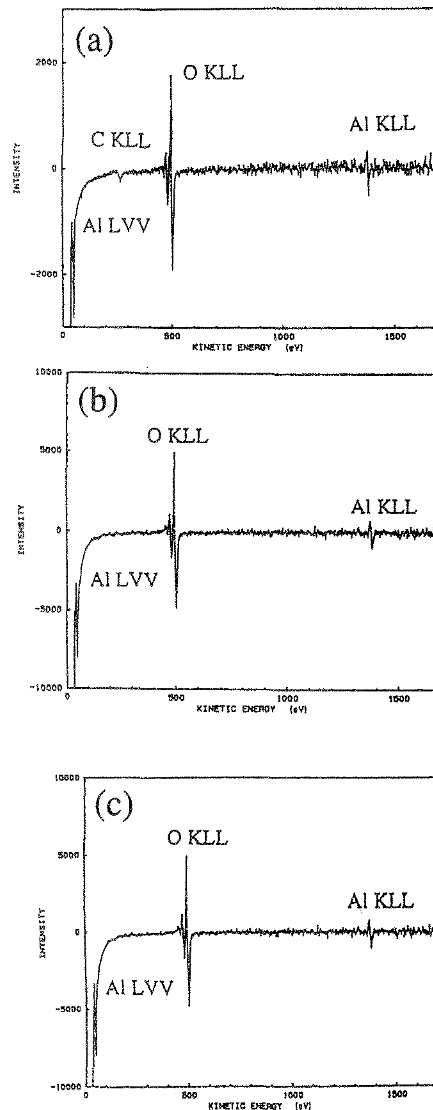

Fig. 6: AES profiles from the thick film(a), particles(b) and the thin film(c).(T=623K)

These exothermic peaks are marked with thin arrows in Fig. 7(a)(b). Small endothermic peak at 460K in Fig. 7(a)(marked with thick arrow) was observed from the thick films deposited at the inlet region. This peak temperature is compared with the previous report[13] due to decomposition of the remaining organic compounds. This indicates the existence of some organics in thick film, which supports the result by the AES analysis(Fig. 6(a)). Because no DTA peaks were observed from the particles deposited at the exit region(Fig. 7(c)), the particles were reduced to Al_2O_3 by passing through the reactor.

[2] Analysis of the output gas from the reactor

The exhaust gas from the reactor under different process conditions was analyzed by means of gas-chromatography. C_3H_6 and C_3H_7OH were detected and their concentrations were determined, using the standard gas samples. Partial pressures of C_3H_6 and C_3H_7OH in the exhaust gas were determined at different reactor temperature and they are plotted in Fig. 8. As the reactor temperature increased, C_3H_6 increased and C_3H_7OH decreased(Fig. 8(a)). Considering the reaction of Eq. (4), it is anticipated that C_3H_7OH decomposes and C_3H_6 is also produced.

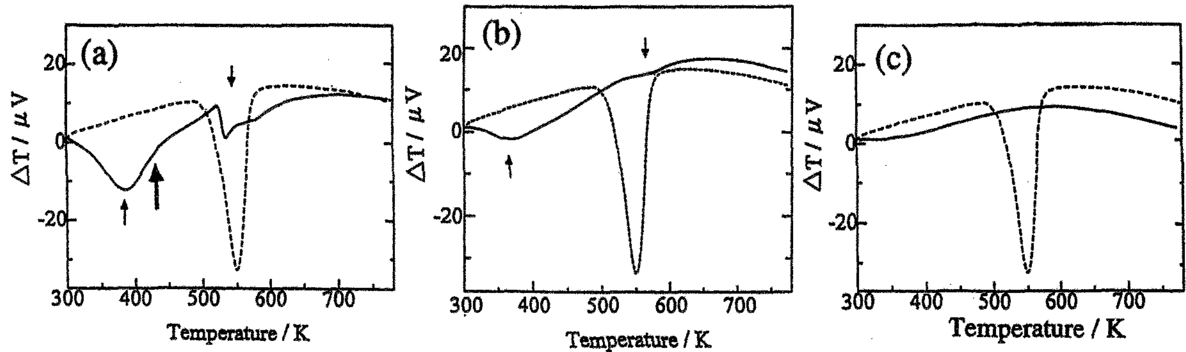

Fig. 7: DTA profiles from the thick film(a), the particles deposited at 0.07m from the inlet(b), and the particles deposited in the exit region(c)(deposited at T=623K).

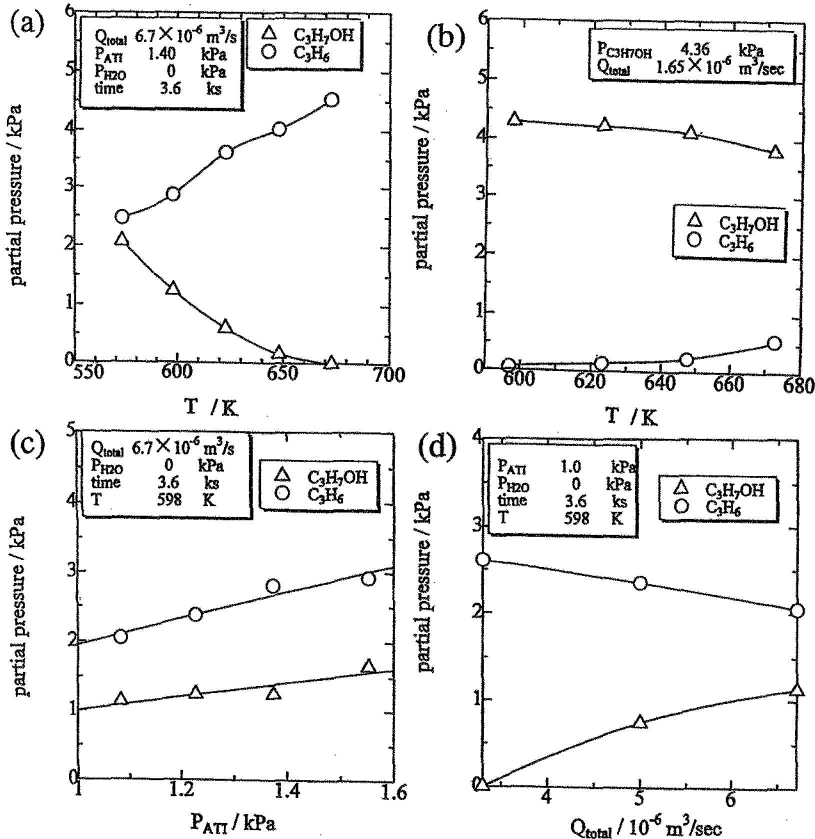

Fig. 8: Partial pressure of C_3H_6 and C_3H_7OH determined by gas chromatography.

(a) : With variation of the reactor temperature,
(b) : Unreacted C_3H_7OH and the produced C_3H_6 (C_3H_7OH was input),
(c): With variation of input ATI partial pressure,
(d): With variation of total gas flow rate.

In order to obtain the decomposition rate of C_3H_7OH at different temperature, gasified C_3H_7OH was input into the reactor. The partial pressures of C_3H_6 and C_3H_7OH in the output gas are plotted in Fig. 8(b). It was seen that the decomposition of C_3H_7OH was not significant, so long as the temperature is less than 650K. Partial pressures of both C_3H_6 and C_3H_7OH increased as the increase of the input ATI partial pressure(Fig. 8(c)).

As the total gas flow rate(Q_T) increased, the partial pressure of C_3H_7OH increased, and that of C_3H_7 decreased(Fig. 8(d)). If it is assumed that the reaction rate for formation of C_3H_6(rection Eq.(2)) is much lower than that of C_3H_7OH(reaction Eq.(1)), the decrease of C_3H_6 production at larger gas flow rate was interpreted to be caused by the increase of linear velocity(decrease of the residence time in the reactor).

[3], The distribution of film thickness

It was observed that the thin film deposited in the range of several millimeter to several centimeters, as the growth rate profiles shown in Fig. 9. The film growth rate was plotted semi-logarithmically, in which their deposition starting positions were set to the origin of the abscissa. It was shown that the distributions in this plots were almost linear, indicating the exponential decrease of the film thickness. It was seen that film deposition at T=598K occurred to the further downstream region and the gradient of the distribution was lower than the other temperature cases. The gradients of the plots at 623K,648K and 673K were almost same, indicating the film growth rates were not determined by the surface reaction rate. The flat distribution at 598K might be due to the difference in the reaction mechanisms, as will be discussed later.

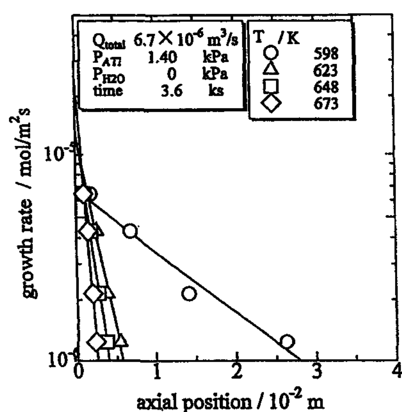

Fig. 9 : Film growth rate distributions at different reactor temperature(T)

IV, Discussion

[1] Consideration of reaction mechanism

It is known[12-14]that alkoxide undergoes the pyrolytic decomposition(Eq.(2)) and the hydrolytic decomposition(Eq.(1)). Reaction mechanism by Schulmann et al.[12]. involves both decomposition reactions. The latter is dominant at low temperature and the former reaction replaces at high temperature. Addition of H_2O into the feed gas was conducted(as shown in the apparatus(Fig. 1)), then the thick film deposition area shifted to the inlet direction[21]. It is also known that the products of the hydrolytic reaction possibly contain organics[14], as a result of reaction Eq. (5), for example.

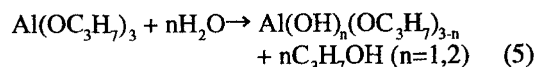

$$Al(OC_3H_7)_3 + nH_2O \rightarrow Al(OH)_n(OC_3H_7)_{3-n} + nC_3H_7OH \ (n=1,2) \quad (5)$$

Existence of carbon in the deposits at the inlet regions(by AES analysis, Fig. 7(a)) might be due to this kind of hydrolytic decomposition of ATI.

Water(H_2O) which initiated and caused the hydrolytic decomposition(Eq. (1)) was not clearly identified in the present study, however, the following possibilities were taken into consideration: (a)H_2O existed in the feed gas in small amount caused the hydrolytic reaction. (b)H_2O was desorbed from ATI(DTA peaks at 380K in Fig. 7(a)(b)), then caused the hydrolytic reactions. The overall reaction (Eq.(1)~Eq.(4)) occurred by the auto-catalytic manner, as discussed in the literature[14].

In the present study, three kinds of decomposition reactions of ATI(Eq. (1)(2)(5)) were considered. Taking account of the DTA results, the transition temperature from the reaction Eq.(5) toEq. (1) was about 460K(Fig. 7(a)). As the temperature increased, the reaction Eq. (2) occurred more, and occurrence of the reaction Eq. (1) became less(Fig. 8(a)).

Difference in the growth rate distributions between at 598K and the higher temperature cases(Fig. 9) was interpreted as follows: The reaction Eq.(3) has not necessarily completed in the deposited thin films at T=598K, while the films obtained at higher than 623K have completed. The cracking of the thick films by heating to 600K(Fig. 5(c)) was also considered to be caused by the decomposition of the remaining organic compounds to C_3H_7OH, C_3H_6, H_2O and other kinds of organics.

[2] Change of the deposits' morphologies

$Al(OH)_3$ molecules or clusters were generated in the gas phase either by pyrolytic reaction or hydrolytic reaction. They coagulated and formed particles which deposited on the substrate. The remaining molecular $Al(OH)_3$ migrated to the substrate by either convection or diffusion. Eventually, it reacted on the substrate surface and thin film was deposited via reaction Eq. (3). As assumed in section III-[2], the pyrolytic decomposition reaction rate for producing C_3H_6 and $Al(OH)_3$ might be lower than that of the hydrolytic reaction, considering the rate has large temperature dependence[14]. Therefore, the pyrolytic decomposition reaction occurred more at the higher temperature region, namely, in the central area of the reactor.

$Al(OH)_3$ particle formation or film deposition occurred in the different regions of the reactor, where wall temperature and concentration of ATI were different. In the intermediate region, they occurred simultaneously. Thin film deposition occurred when ATI concentration reduced in the down stream region. Distribution of thin film deposition rates was determined by the mass transfer of ATI(and its decomposed species), and caused the exponential decrease of the growth rate along the axial direction[22].

V,Conclusion

Vaporized ATI was fed into a horizontal tubular reactor under various conditions of substrate temperature, gas flow rate and gas compositions. Observation of deposits' morphologies, analysis of the particles and films were conducted. Following conclusions were obtained from the experimental results:

1, At the inlet low temperature region below 450K, thick film deposited, in which carbon was detected. Hydrolytic decomposition reaction of ATI might be related to formation of the deposition.

2, The $Al(OH)_3$ molecules or clusters produced in the gas phase coagulated to form particles or migrated to the substrate and deposited thin films. Their occurrence was dependent on the positions in the reactor, namely, the temperature and concentration in the reactor.

3. The pyrolytic reaction occurred at the higher temperature, producing the larger amount of C_3H_6. The production rate decreased at larger gas flow rate.

4, Amorphous thin films deposited in the downstream region. Their thickness decreased exponentially along the axial direction of the reactor. The growth rate distribution at T=598K was much flatter than the high temperature cases, because of the difference in deposition reaction mechanism.

VI, References

1, K.K.Yee, Int. Met. Rev., [1] (1978) 19.
2,H.J.Viljoen, J.J.Thiart and V.Hlavacek, AIChE. J. 40 [6] (1994) 1032.
3, C.Dhanavantri, R.N.Karekar and V.J.Rao., Thin Solid Films, 127 (1985) 85.
4, M.Okada, T.Ido and A.Moriyama, Denki Kagaku, 53 (1985) 802.
5, J.Saraie, J.Kwon and Y.Yodogawa, ibid., 132 (1985) 890.
6, H.Mutoh, Y.Mizokami, H.Matsui, S.Hagiwara and M.Ino, J. Electrochem. Soc., **122** (1975) 987.
7, Pauer,G et al., J. Hard Met., (1986) 165.
8, Sladek,K.J. et al., Proc. 3rd. Conf. On CVD p. 215 (1972)
9, J.A.Aboaf, J.Electrochem. Soc., 114 (1967) 948.
10, T.Go and K.Sugimoto, J. Jpn. Inst. Met., 56 (1992) 184.
11,R.W.J.Morssinkhof, T.Fransen, M. M. D. Heusinkveld and Gellings, Symp. Proc. Mater. Res. Soc., 168 (1990) 125.
12, G.P.Schulman, M.Trusty and J.H.Vickers, J.Org.Chem., 28 (1963) 907.
13, D.C.Bradley, Chem. Rev., 89 (1989) 1317.
14, R.Xu, J.Mater. Res., 10 [10] (1995) 2536.
15, A.C.Adams and C.D.Capio, J. Electrochem. Soc., 126 (1979) 1042.
16, S.B.Desu, J.Am.Ceram.Soc., 72 (1989) 1615.
17, G.B.Raupp, F.A.Shemansky and T.S.Cale, J.Vac.Sci.Tech. B10 (1992) 2422.
18, L.S.Hong and H.Komiyama, J.Am.Ceram.Soc., 74 (1991) 1597.
19, N.Yoshikawa and A.Kikuchi, J.Mater.Res., 10 [11] (1995) 2801.
20, R.H.Hurt and M.D.Allendorf, AIChE.J., 37 [10] (1991) 1485.
21, S.Takamura, Master Thesis at Tohoku Unversity (1996)
22, H.Komiyama, H.J.Kim, T.Osawa and Y.Egashira, Ceramics 26 [8] (1991) 7593.